SCIENTIFIC REPORTS

OPEN

SUBJECT AREAS:
TUMOUR SUPPRESSORS
CANCER PREVENTION
MACROAUTOPHAGY

Received
16 September 2013

Accepted
5 March 2014

Published
24 March 2014

Correspondence and requests for materials should be addressed to Y.S. (shidoji@sun.ac.jp)

Induction of nuclear translocation of mutant cytoplasmic p53 by geranylgeranoic acid in a human hepatoma cell line

Chieko Iwao & Yoshihiro Shidoji

Molecular and Cellular Biology, Graduate School of Human Health Science, University of Nagasaki, Academy Hills 1-1-1, Nagayo, Nagasaki 851-2195, Japan.

Mutant p53 proteins in human hepatoma cell lines such as HuH-7 (Y220C) and PLC/PRF/5 (R249S) accumulate in the cytoplasm, and lose their transcriptional function. Geranylgeranoic acid (GGA) is a naturally occurring acyclic diterpenoid that induces cell death in both cell lines, but not in HepG2 cells harboring wild-type p53. Here, we demonstrate that micromolar concentrations of GGA induce a rapid nuclear translocation of cytoplasmic p53 in both p53-mutant cell lines and p53 knockdown attenuates GGA-induced cell death in HuH-7 cells. Cell-free experiments demonstrate that GGA is able to release 670-kD p53-containing complexes from putative huge macromolecular aggregates in post-mitochondrial fractions as revealed on blue-native gradient PAGE. Among several p53-target genes tested, GGA upregulates *PUMA* gene expression, and ivermectin, an inhibitor for importin α/β, blocks GGA-induced nuclear translocation of cytoplasmic p53 and suppresses GGA-induced upregulation of *PUMA* mRNA levels in HuH-7 cells. Taken together, these data suggest that GGA treatment stimulates a nuclear translocation of mutant p53 through its dissociation from cytoplasmic aggregates, which may be essential for GGA-induced cell death.

The structure, function, and clinical significance of the p53 tumor suppressor protein in oncology have been previously described in extensive detail[1,2]. The p53 transcription factor responds to diverse stresses (including DNA damage, overexpressed oncogenes, and various metabolic limitations) to regulate many target genes that induce cell-cycle arrest (e.g., *p21* or *CDKN1A* as provided by the HUGO Nomenclature Committee [HGNC]), cell death (e.g., *PUMA*, p53-upregulated modulator of apoptosis, or *BBC3*, BCL2 binding component 3, as indicated by HGNC), respiration (e.g., *SCO2,* synthesis of cytochrome *c* oxidase-2), and inhibition of glycolysis (e.g., *TIGAR*, TP53-induced glycolysis and apoptosis regulator)[3]. All of these p53 targets have been linked to p53-mediated prevention of tumorigenesis.

Among these targets, the *PUMA* gene is particularly interesting in terms of cancer prevention, as the gene was identified as a p53-dependent potent inducer of mitochondria-mediated cell death in diverse tissues and cell types[4]. PUMA is one of the bcl-2 homology domain 3 (BH-3)-only proteins, which induce the mitochondrial outer membrane permeability transition. Therefore, overexpression of PUMA causes hyperproduction of reactive oxygen species from mitochondria, resulting in mitochondria-mediated cell death. Although PUMA is well established as an essential component of p53-mediated apoptosis[4], PUMA also contributes to induction of autophagy during p53-dependent cell death[5].

Almost half of clinical cancers have been reported to harbor mutations in the *p53* gene[2]. In clinical cancers, most mutation hotspots reside in the core or DNA-binding domain of p53. Mutations in the core domain give rise to either loss of function or gain of function in p53 transcriptional activity. In terms of cellular fate of the p53 mutations, mutations in the core domain can be subdivided into two groups with distinct functional consequences: p53 enhanced degradation or p53 cytoplasmic accumulation[6,7].

Several p53-interacting proteins have been reported to be involved in its cytoplasmic sequestration, blocking it from degradation as well as restricting its access to the nuclear compartment, where p53 plays a role in transcription. Among the p53-interacting proteins, the 250-kDa CUL9 (previously named PARC, p53-associated, parkin-like cytoplasmic protein, by HGNC), a member of the cullin family and a potential E3 ubiquitin ligase[8], is

one of the major players that sequester p53 in cytoplasm. The CUL9 N-terminus binds the C-terminus of p53 and forms an approximately 1-MDa multi-protein complex that then blocks transport of cytosolic p53 into the nucleus, thus retaining p53 in cytoplasm[9].

p53 has attracted much attention over recent years in the autophagy field, as p53 exhibits dual distinct roles in autophagy[10]. p53 transactivates the autophagy-related gene *DRAM* (damage-regulated autophagy modulator)[11], which is required for p53's ability to induce autophagy[12]. Cytoplasmic p53 has been shown to repress autophagy via poorly characterized mechanisms[13].

Geranylgeranoic acid (GGA), which consists of four isoprene units and has a carboxylic group at its terminus, is found in several medicinal herbs[14]. In the past decade, 4,5-didehydroGGA has been proven to suppress carcinogenesis in experimental animal models[15] and shown to be an efficient prevention chemical against second primary hepatoma in phase I/II/III clinical trials[16,17]. We previously examined the molecular mechanism underlying second primary hepatoma-preventive action of the polyprenoic acid, and showed that GGA induces cell death of human hepatoma-derived HuH-7 and PLC/PRF/5 cells, both of which have p53 protein mutated in the core domain. In contrast, cell death was not observed after GGA treatment of wild-type p53 homozygote cells, such as mouse primary hepatocytes and human hepatoblastoma-derived HepG2 cells, in FBS-free medium[14].

During GGA-induced cell death, HuH-7 cells display dissipated inner membrane potential of mitochondria[18,19]. This mitochondria-involved cell death showed characteristics of apoptosis, such as chromatin condensation as revealed by Hoechst staining. However, caspase inhibitors were unable to block GGA-induced cell death[18]. These results suggest that GGA-induced cell death is not a typical apoptotic process, but might be a caspase-independent and non-necrotic cell death. Recently, we found that GGA provides substantial accumulation of autophagosomes under serum starvation conditions in human hepatoma cells[19]. Autophagy-inducing stimuli should cause the depletion of cytoplasmic p53, which in turn is required for the induction of autophagy[13].

In this context, we speculated that the mutant p53 accumulated in the cytoplasm of HuH-7 cells might disturb GGA-induced accumulation of autophagosomes. In other words, GGA should act on the accumulated p53 to remove it from the cytoplasmic compartment, translocating the cytoplasmic p53 into the nucleus and potentially reactivating the mutant p53 to induce cell death. In the present paper, we found a rapid nuclear translocation of p53 after GGA treatment of HuH-7 cells. To evaluate the mechanism by which GGA translocates mutant cytoplasmic p53 to the nucleus, we analysed native forms of the cytoplasmic p53 by applying GGA to post-mitochondrial fractions in a cell-free system.

Results

Mutant p53 is involved in GGA-induced cell death of HuH-7 cells. As repeatedly reported, GGA induced cell death in HuH-7 cells in a dose-dependent manner (Figure 1a). In order to know whether mutant p53 is involved in GGA-induced cell death, we conducted p53 knockdown experiment. Although the cellular levels of p53 in HuH-7 cells transfected with p53 siRNA were not completely knocked down, a significant down-regulation of cellular p53 levels was observed and GGA treatment did not change the cellular p53 levels (Figure 1b). However, GGA-induced cell death was significantly blocked in p53-siRNA-treated cells (Figure 1c), indicating that p53 knockdown indeed rescued cell death induced by GGA, confirming that GGA works through the mutant p53 in HuH-7 cells.

Mutant p53 relocates from the cytoplasm to the nucleus by GGA treatment. As it was proved that the mutant p53 might play a role in GGA-induced cell death in HuH-7 cells, we speculated that GGA might translocate the mutant p53 into the nucleus to transactivate its target genes. As shown in Figure 2a, the cellular accumulation of the

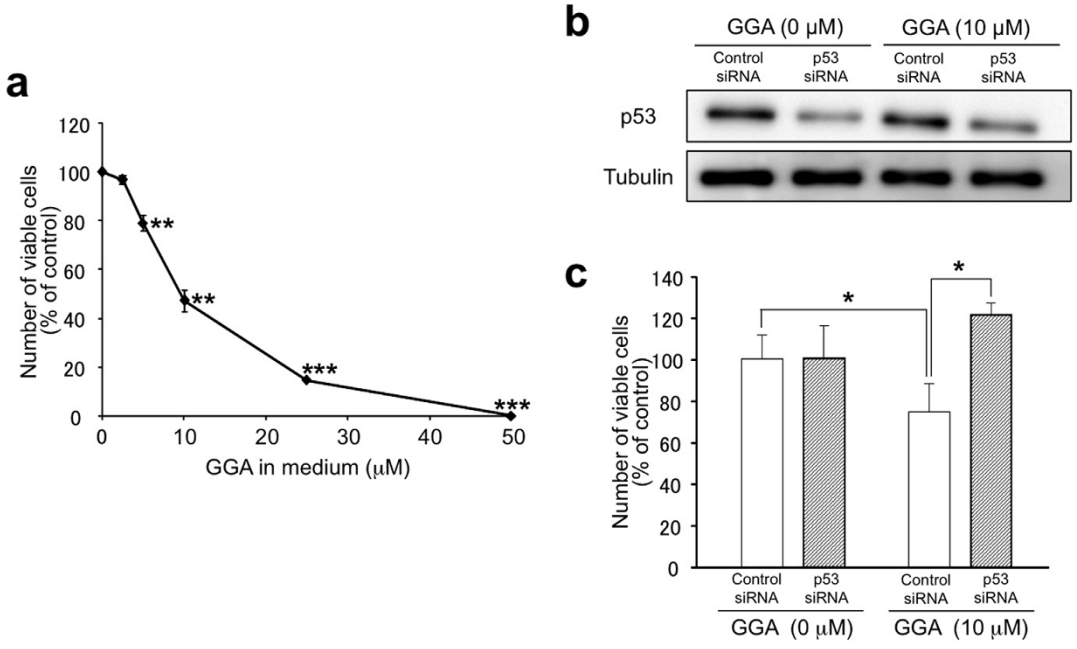

Figure 1 | Mutant p53 is involved in GGA-induced cell death of HuH-7 cells. (a) Viable cells were counted using the Trypan Blue dye-exclusion method at 24 h after treatment with 0, 2.5, 5, 10, 25, or 50 μM GGA. The experiments were repeated 3 times. Values are the means ± SE ($n = 3$). (b) Cellular p53 protein levels in HuH-7 cells are shown at 8-h GGA treatment after 96-h pretreatment with control siRNA or p53 siRNA. Whole cell lysates were prepared and p53 levels were analysed by western blotting. Tubulin-β was used as a loading control. (c) HuH-7 cells were treated with 0 (vehicle control) or 10 μM of GGA for 24 h after 96-h pretreatment with control siRNA or p53 siRNA. And then viable cells were counted by Trypan Blue dye-exclusion method. Values are the means ± SE ($n = 4$). The asterisks (*, ** and ***) indicate statistically significant changes ($p < 0.05$, 0.01 and 0.001) respectively as determined by the Student's t-test.

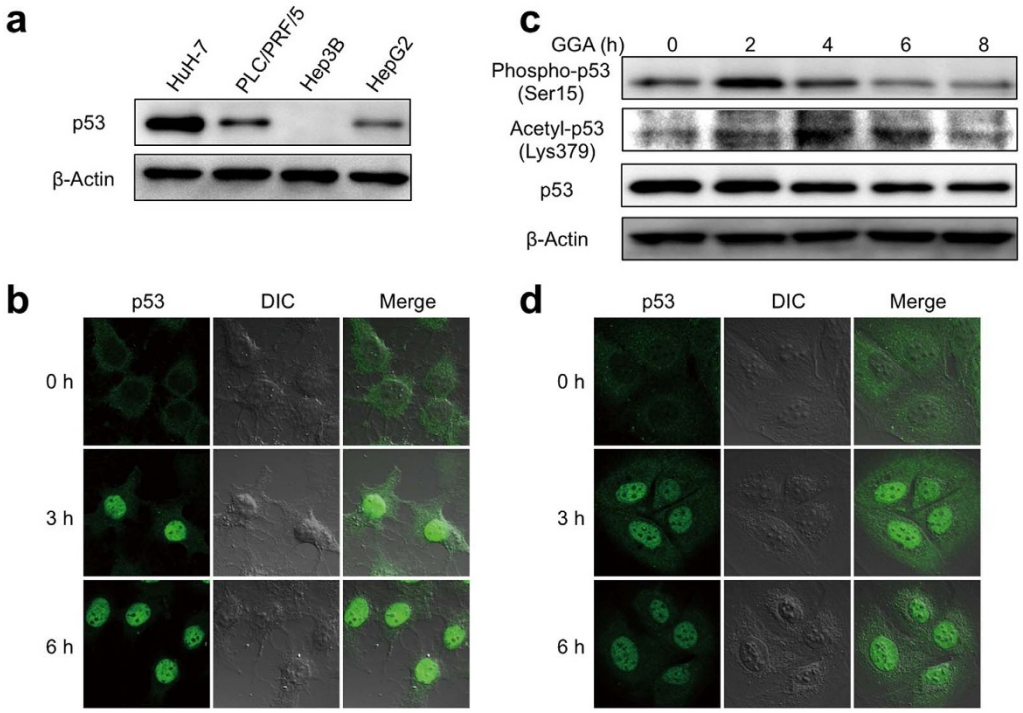

Figure 2 | Mutant p53 is relocated from the cytoplasm to the nucleus by GGA. (a) Cellular p53 protein level in HuH-7, PLC/PRF/5, Hep3B, and HepG2 cells. Whole-cell lysates were prepared and the p53 level was analysed by western blotting. (b) HuH-7 cells were treated with or without 20 μM of GGA for 3 and 6 h. Green fluorescence indicated the distribution of p53. (c) HuH-7 cells were treated with or without 20 μM of GGA for 2, 4, 6, and 8 h. Whole-cell lysates were prepared and phospho-p53 (Ser15), acetyl-p53 (Lys379), and p53 levels were analysed by western blotting. Total β-actin was used as a loading control. (d) PLC/PRF/5 cells were treated with or without 20 μM of GGA for 3 and 6 h. Green fluorescence indicated the distribution of p53.

mutant p53 was observed in HuH-7 cells under basal conditions, compared with three other hepatoma cell lines. We next investigated changes in the subcellular localization of the accumulated p53 protein during GGA treatment. At first, we measured GGA-induced changes in the subcellular distribution of p53 by subcellular fractionation followed by western blotting. Although we found that GGA treatment decreased the cytoplasmic p53, we failed to demonstrate GGA-induced nuclear accumulation of p53 (Supplementary Figure S1). However, as clearly shown in Figure 2b, an immunofluorescence technique revealed that the p53 protein in non-treated HuH-7 cells accumulated as reticular forms in the cytoplasm and was completely excluded from the nucleus, whereas GGA treatment for 3 h induced a dramatic subcellular shift of the p53 protein from the cytoplasm to the nucleus. At 6 h after addition of GGA, the cytoplasmic levels of p53 became undetectable. In other words, almost all of the cellular p53 concentrated in the nucleus and no p53 remained in the cytoplasm 6 h after GGA treatment. Furthermore, transient post-translational modifications of p53, such as Ser-15 phosphorylation[20] and Lys-379 acetylation[21], indicators for nuclear translocation, were induced by addition of GGA at 2 h (Figure 2c).

We next evaluated whether GGA-induced nuclear translocation was observed in PLC/PRF/5 cells, in which a lower cellular accumulation of mutant p53 was detected (Figure 2a). PLC/PRF/5 cells accumulated p53 in the cytoplasm in normal culture conditions, similar to HuH-7 cells (Figure 2d). PLC/PRF/5 cells also showed translocation of p53 from the cytoplasm to the nucleus by 3 h of GGA treatment, and a trivial amount of p53 remained in the cytoplasm 6 h after GGA treatment (Figure 2d).

GGA-induced changes in native forms of p53 in the cytoplasmic space. To elucidate the mechanism by which cytoplasmic p53 translocates to the nucleus upon GGA treatment, we used the post-mitochondrial fraction to examine a direct effect of GGA on native forms of p53 in the cytoplasm, as mutant p53 accumulates mostly in this fraction in HuH-7 cells, but less either in the cytosol or mitochondria fraction (Supplementary Figure S2).

Figure 3a clearly shows large native forms of p53 in the post-mitochondrial fractions using blue-native (BN)-gradient PAGE. Unfortunately, we failed to detect major p53-positive bands, but observed a faint, vague, and broad 670-kD band on the blot of the BN-gradient gel with control post-mitochondrial fractions, indicating that most of the cytoplasmic p53 could be too large in size to penetrate into the gradient gel. We were able to detect relatively dense bands of a p53-containing complex at a molecular size of around 670 kD with samples incubated with GGA (Figure 3a). More importantly, the total amount of p53 that penetrated into the BN-gradient gel increased in a GGA concentration-dependent manner (Figure 3a), whereas in ordinary SDS-PAGE, the total amount of p53 stayed constant in post-mitochondrial samples incubated with any concentrations of GGA (Figure 3b). Interestingly, a 210-kD complex of p53 (the molecular size equivalent to a p53 homotetramer) was evident in all GGA-treated samples (Figure 3a). Such changes were not observed with HepG2 cells (wild-type p53 control cell line).

Because of the relatively poor resolution of the BN-gradient PAGE, we next used cross-linking SDS-PAGE to examine GGA-induced changes in native forms of p53. In HuH-7 post-mitochondrial preparations incubated with increasing concentrations of GGA, a few major bands of p53-positive complexes larger than 250 kD were also detected by cross-linking SDS-PAGE (Figure 3c). Moreover, unlike the BN-gradient PAGE, a band of p53 monomer was detected in GGA-containing samples. These results were not observed with post-mitochondrial fractions of HepG2 cells and no GGA-induced changes were detected on the cross-linking SDS-PAGE membrane using HepG2 cells.

Both BN-gradient PAGE and cross-linking SDS-PAGE experiments strongly indicate that in HuH-7 cells prior to GGA treatment,

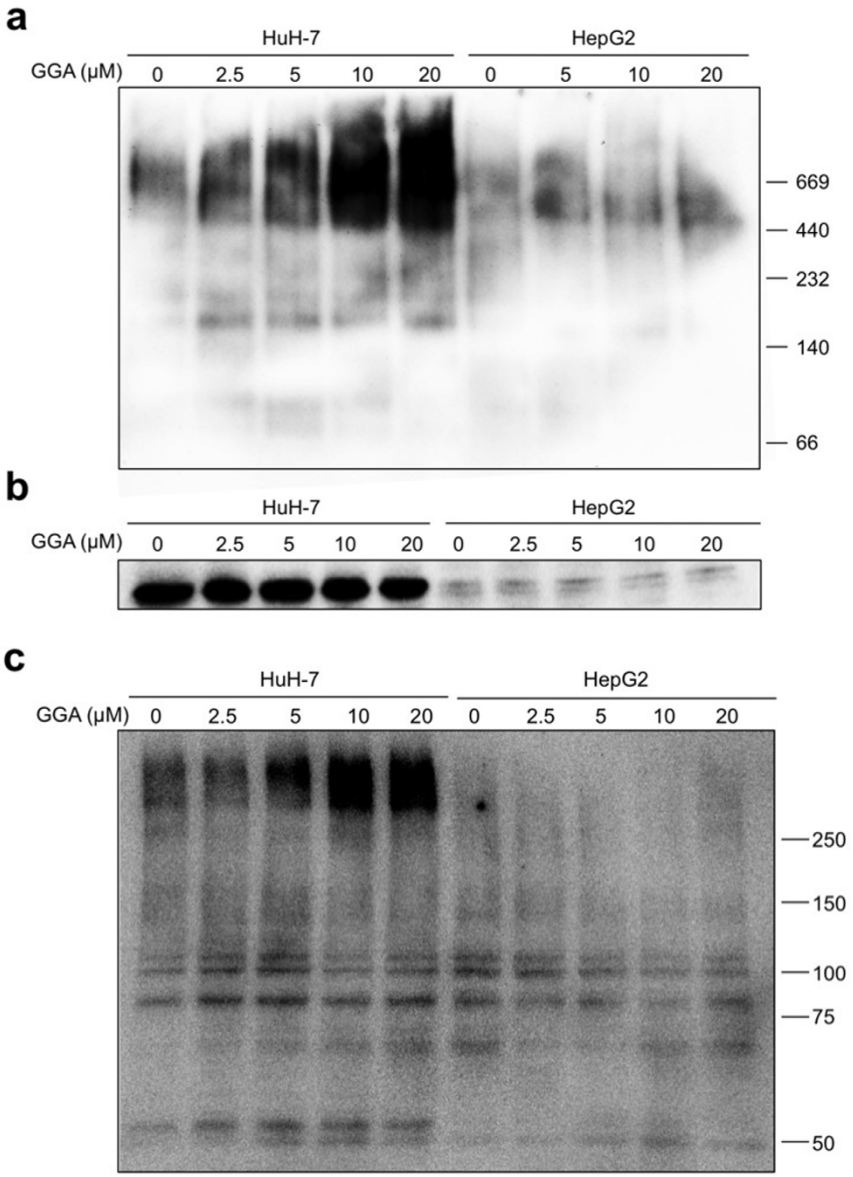

Figure 3 | GGA-induced changes in native forms of p53 in the post-mitochondrial fraction. The post-mitochondrial fractions from HuH-7 (p53 Y220C) and HepG2 (p53 WT) cells were incubated with GGA (0–20 μM) at 4°C overnight. Samples (3.75 μg protein per each lane) were subjected to BN-gradient PAGE (a) or ordinary SDS-PAGE (b), followed by western blotting with anti-p53. (c) Aliquots (5 μg protein per each lane) of samples were subjected to cross-linking SDS-PAGE followed by western blotting with anti-p53.

most of the cytoplasmic p53 may exist as huge complexes larger than 670 kD, which do not enter the BN-gradient gel, and cell-free treatment with GGA reduced the molecular size of the cytoplasmic p53-containing complex down to 670 kD and less.

p53 is released from putative huge complexes with GGA treatment. The GGA-induced p53 complex of >250 kD disappeared from the gel when the same experiment was conducted with the cytosolic fraction instead of the post-mitochondrial fraction (Figure 4a), suggesting that the cytoplasmic p53 forms a huge multi-protein complex that sediments after 105 000 *g* for 90 min or sticks to organelles, such as the endoplasmic reticulum.

Studies from the literature have reported one of the possible huge complexes of cytoplasmic p53 is the CUL9/PARC multi-protein complex, with a molecular size of approximately 1 MD[22]. In the post-mitochondrial fractions from HuH-7 cells, p53 was able to successfully co-immunoprecipitate with anti-PARC in the absence of GGA (Figure 4b), indicating that part of the cytoplasmic p53 might be complexed with PARC. Interestingly, the amount of p53 that co-immunoprecipitated with PARC was reduced after cell-free incubation of GGA in a concentration-dependent manner, indicating that p53 could be directly released from the PARC complex by addition of GGA in a cell-free system.

We tested another possibility for the large p53-containing complexes involving the interaction of p53 with microtubules, based on the theory in which cytoplasmic p53 forms a tetramer when p53 moves into nuclei via microtubules[23]. As described above, cross-linking SDS-PAGE followed by western blotting with anti-p53 revealed that GGA induced the p53 complex of over 250 kD, as shown in Figure 3c and Figure 4c. When this membrane was re-probed with an anti-β-III-tubulin antibody, co-existence of tubulin with p53 in the >250 kD complex was detected, but most of β-III-tubulin was not detected in the control post-mitochondrial fraction probably because of cross-linking of α/β-subunit assembly by tubulin filaments (Figure 4d).

GGA treatment upregulates *PUMA* gene expression in HuH-7 cells. GGA has been repeatedly reported to induce cell death in HuH-7 cells[18,19,24]. PUMA is a critical mediator of p53-dependent

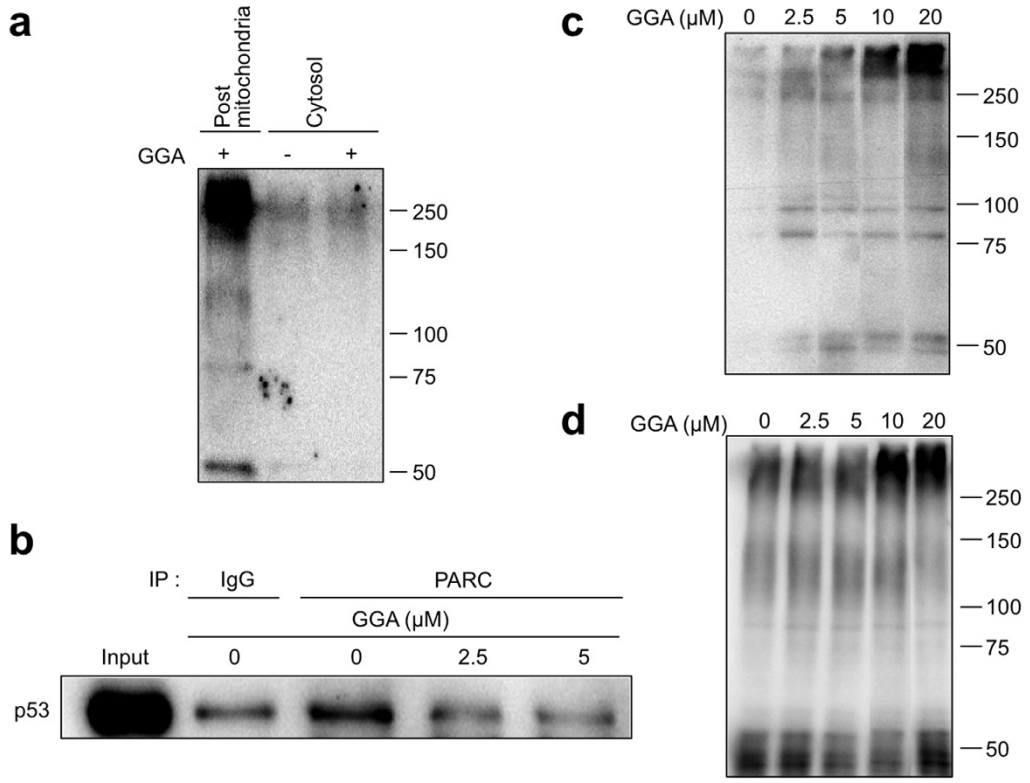

Figure 4 | p53 is released from putative huge complexes after GGA treatment. (a) The post-mitochondrial and cytosolic fractions from HuH-7 cells were incubated with or without GGA (20 μM) at 4°C overnight. Samples (5 μg protein) were subjected to cross-linking SDS-PAGE followed by western blotting with anti-p53. (b) The post-mitochondrial fraction from HuH-7 cells was incubated with GGA (0–5 μM) at 4°C overnight, followed by immunoprecipitation with the anti-PARC antibody (PARC) or an equal amount of non-immune rabbit IgG (IgG). The immunoprecipitates were analysed by immunoblotting with an anti-p53 antibody. 12.5% of the input was used for immunoblotting (Input). The post-mitochondrial fraction from HuH-7 cells was incubated with GGA (0–20 μM) at 4°C overnight. Aliquots (5 μg protein) of samples were subjected to cross-linking SDS-PAGE followed by western blotting with anti-p53 (c) and the membrane was reproved with anti-β-III-tubulin (d). Images of panel (c) and (d) were cropped from single each blot shown in Supplementary Figure S3.

and -independent cell death[4]. Therefore, we investigated dose-dependent changes in *PUMA* mRNA levels during GGA-induced cell death in HuH-7 cells. GGA upregulated *PUMA* mRNA levels in a dose-dependent manner, increasing levels from 1.3-fold higher than controls at 2.5 μM, up to 15.7-fold higher than controls at 20 μM at 8 h (Supplementary Figure S4a). We then conducted a time-course experiment using 20 μM GGA (Figure 5a). Treatment with 20 μM GGA clearly induced expression of *PUMA* mRNA levels as early as 2 h after treatment. At 8 h, the levels reached almost 17.7-fold higher than control levels. In contrast, the mRNA levels of all other p53-target genes tested, including *TIGAR*, *DRAM*, *p21*, and *SCO2*, were not significantly induced after 24 h of GGA treatment, except that the cellular p21 mRNA levels were marginally up-regulated at this time point (Figure 5a). The cellular level of PUMA protein relative to β-actin was slightly higher after 4 h of 20 μM GGA treatment, which occurred slightly after GGA induction of the *PUMA* mRNA level (Figure 5a, Supplementary Figure S4b). The mitochondrial level of PUMA protein relative to porin was also increased at 6 h (Supplementary Figure S4b).

To examine whether GGA-induced upregulation of *PUMA* gene expression in HuH-7 cells was associated with mutation of the *p53* gene, we next evaluated the effects of GGA on *PUMA* gene expression in several other human hepatoma cell lines. Other cell lines, such as PLC/PRF/5 (mutant p53, R249S) and HepG2 (wild-type p53) did not show upregulation of *PUMA* mRNA levels after GGA treatment, except for Hep3B (p53-null) cells that showed an upregulation of 5-fold at 4 h (Supplementary Figure S4c), indicating that the dramatic effect of GGA on *PUMA* gene expression was highly specific for HuH-7.

Nuclear translocation of mutant p53 upregulates *PUMA* mRNA levels in HuH-7 cells. We next speculated whether GGA-induced nuclear translocation of p53 was involved in GGA-induced upregulation of *PUMA* mRNA levels in HuH-7 cells. We used ivermectin, a newly established inhibitor specific against importin α/β-mediated nuclear import[25], to block GGA-induced nuclear translocation of p53. The drug suppressed GGA-induced nuclear translocation of p53 in HuH-7 cells and most of the cytoplasmic p53 remained around the perinuclear regions after 3 h of treatment with GGA (Figure 5b). Furthermore, we found that ivermectin also significantly suppressed GGA-induced upregulation of *PUMA* mRNA, although *PUMA* mRNA levels were still up-regulated by 4.5-fold with GGA-induction in the presence of ivermectin (Figure 5c).

These findings led us to speculate whether GGA-induced nuclear-translocated mutant p53 is able to function in the transactivation and upregulation of *PUMA* gene expression. We next evaluated the impact of GGA on transcriptional activation of the *PUMA* gene using p53 response elements. In a luciferase reporter assay using a standard p53-responsive consensus sequence, GGA treatment did not upregulate reporter gene expression, and even downregulated it in a dose-dependent manner (Supplementary Figure S5a). In contrast, the reporter assay using the p53-responsive 5′-upstream regulatory region of the *PUMA* gene demonstrated GGA-induced upregulation

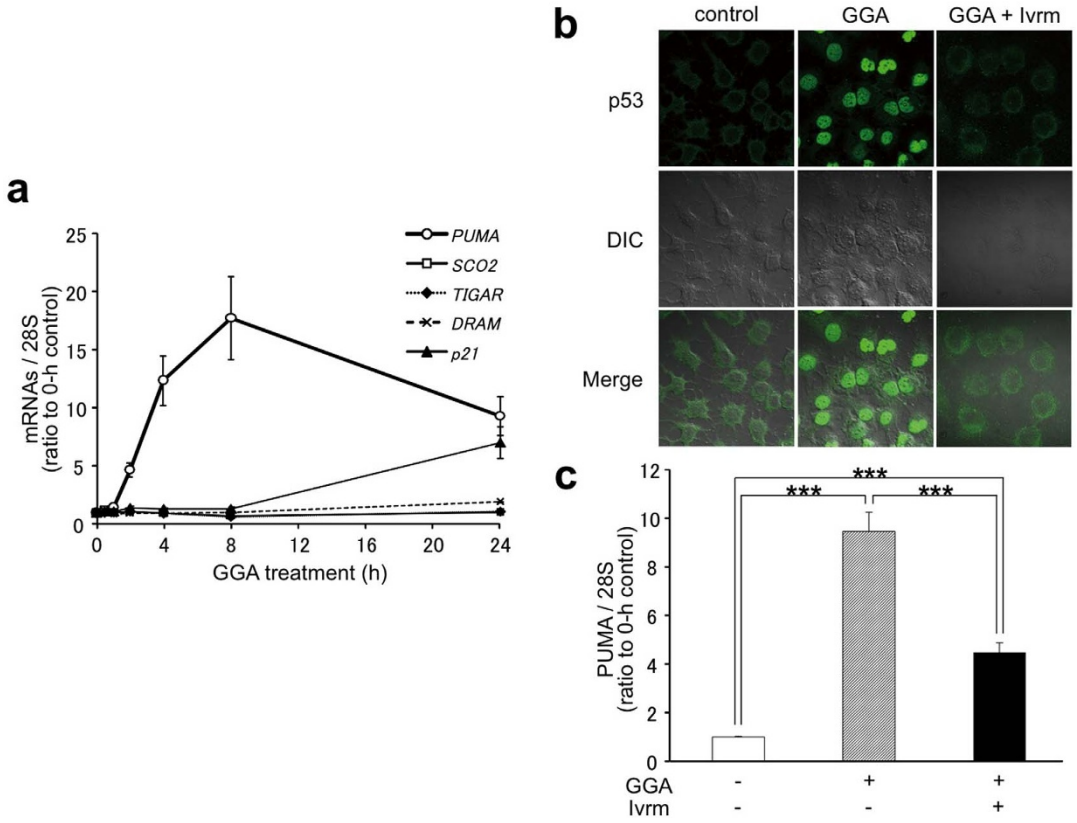

Figure 5 | Nuclear translocation of mutant p53 upregulates *PUMA* gene expression. (a) HuH-7 cells were treated with or without 20 μM of GGA for 0.5, 1, 2, 4, 8, and 24 h, and total mRNA was extracted to analyse *PUMA*, *SCO2*, *TIGAR*, *DRAM*, and *p21* mRNA expression by quantitative RT-PCR. For *PUMA*, each point represents the mean ± SE of six independent experiments, while data points for all other genes represent the mean ± SE of three independent experiments. (b) HuH-7 cells were cultured under the following conditions: no treatment (control), 20 μM GGA for 3 h (GGA), or 20 μM GGA with ivermectin, a specific inhibitor of importin, for 3 h (GGA + Ivrm). Green fluorescence indicated the distribution of p53. (c) HuH-7 cells were cultured under the conditions as in (b), and total mRNA was extracted to analyse *PUMA* mRNA expression by quantitative RT-PCR.

of the reporter gene in a time-dependent manner (Supplementary Figure S5b).

Discussion

GGA is a cancer-preventive diterpenoid that has been recently shown to induce mitochondria-mediated cell death with an incomplete autophagic response in HuH-7 cells[19]. In the present study, we have clearly demonstrated that mutant p53 that accumulates in the cytoplasm of human hepatoma cell lines, including HuH-7 and PLC/PRF/5, is translocated to the nuclear compartment immediately after treatment with GGA. Furthermore, p53 knockdown experiment clearly demonstrated that the mutant p53 might play an essential role in GGA-induced cell death. Therefore, prior to scrutiny at the molecular level as to the downstream signals of p53 occur in the GGA-treated hepatoma cell lines, it may be important to determine how GGA translocates cytoplasmic p53 to the nucleus.

In general, cytoplasmic accumulation of mutant p53 can be caused both by blocking proteasomal degradation of p53 as mediated by its binding with MDM2, a p53-specific E3 ubiquitin protein ligase, and by sequestration of p53 via formation of large p53-containing aggregates with other p53-binding cytoplasmic proteins, such as CUL9/PARC[26], heat-shock proteins (HSPs)[27,28], and other proteins. It is reasonable to speculate that GGA that penetrated in the cytoplasm of HuH-7 cells may be able to change native forms of cytoplasmic p53 from putative huge aggregates (sedimenting at 105 000 *g* and 348 900 *g* for 90 min; Figure 4a and Supplementary Figure S2, respectively) to a potent transportable form, which is likely composed of at least three components, such as tetrameric p53, motor proteins such as dynein, and subunits of microtubules[23]. Indeed, in cell-free experiments in the present study, we were able to demonstrate that GGA transforms native forms of cytoplasmic p53 from non-penetrating huge aggregates to penetrating approximate 670-kD complexes on both BN-gradient PAGE (Figure 3a) and crosslinking SDS-PAGE (Figure 3c) in a dose-dependent manner. Furthermore, β-III-tubulin was shown to be crosslinked to these complexes in the presence of GGA in a dose-dependent manner (Figure 4d). We also showed co-precipitation of cytoplasmic p53 with CUL9/PARC using the post-mitochondrial fraction and GGA-dependent dissociation of p53 from CUL9/PARC. In this context, one can easily speculate that these cell-free effects of GGA on native forms of cytoplasmic p53 may enable p53 to be transiently Ser-15 phosphorylated[29] and Lys-379 acetylated[30] (Figure 2c).

In parallel with stimulating nuclear translocation of p53, GGA also induced a dramatic upregulation of the *PUMA* gene, a key regulator of p53-mediated cell death, at the mRNA and protein levels in HuH-7 cells. Indeed, mitochondrial PUMA protein level increased 2–3-fold at 6 h after GGA treatment, which reasonably explains our previous findings that GGA efficiently dissipates the mitochondrial inner membrane potential and induces hyper-production of superoxide at mitochondria[18,31]. Furthermore, GGA-induced upregulation of *PUMA* mRNA levels is clearly dependent on nuclear translocation of p53, as ivermectin, a specific inhibitor of importin $\tilde{\alpha}\beta$, blocked GGA-induced nuclear translocation of p53 and also partially suppressed GGA-induced upregulation of *PUMA* mRNA levels. Together these findings strongly suggest that GGA may reactivate the mutant p53 (Y220C) as a transcription factor via its nuclear translocation. However, none of the mRNA levels of p53 target genes tested in this study, including *SCO2*, *TIGAR*, *DRAM*, and *p21*, were upregulated by GGA treatment, suggesting that GGA-induced transcriptional activa-

tion is specific for the *PUMA* gene in HuH-7 cells. In considering that the transactivation effect of GGA is specific for the *PUMA* gene, it is worth mentioning that p53-mediated transcription of the p53-responsive consensus sequence was inversely suppressed by GGA treatment in a dose-dependent manner (Supplementary Figure S5a), indicating that the nuclear-translocated mutant p53 behaved as a dominant negative mutant against the consensus sequence in p53 heterozygotic HuH-7 cells (unpublished results). However, the nuclear-translocated p53 transactivated a reporter gene downstream of the p53-responsive 5′-upstream regulatory region of the *PUMA* gene after GGA treatment in a time-dependent manner in HuH-7 cells (Supplementary Figure S5b), suggesting that the mutant p53 (Y220C) still retained its ability to play a role in transcription of the *PUMA* gene, which contains a low affinity BS1 p53 response element[32].

On the contrary, PLC/PRF/5 cells did not upregulate *PUMA* gene expression after GGA treatment (Supplementary Figure S3c), although the cells showed translocation of cytoplasmic p53 to the nucleus after GGA treatment, similar to HuH-7 cells (Figure 2). In this case, the nuclear-translocated p53 does not seem to transactivate the *PUMA* gene. While the Y220C mutation of p53 in HuH-7 cells resides at the beginning of the loop that connects β-strands S7 and S8 of the β-sandwich in the core domain of p53, the R249S mutation in PLC/PRF/5 cells is located at a DNA-contact region of the α-helix of the DNA-binding domain[33]. The former mutant is categorized into class *iv*, with a determinant structural region of the β-sandwich, which shows less affinity to DNA (35–75% of wild type), but the latter mutant belongs to class *ii*, with a determinant structural region of the D-binding region, which completely loses binding affinity to DNA[34]. Therefore, we speculate that PLC/PRF/5 cells might be no longer able to transactivate the *PUMA* gene, even though GGA translocated cytoplasmic p53 to the nuclear compartment. Inasmuch as GGA induces cell death in PLC/PRF/5 cells without induction of the *PUMA* gene, we are speculating that PUMA may not be solely responsible for GGA-induced cell death, but may be rather supportive for the cell death in HuH-7 cells.

Finally, we should provide a perspective on a link between nuclear translocation of cytoplasmic p53 and the GGA-induced autophagic response in HuH-7 cells[19]. Given that PUMA is able to induce autophagy[5], GGA-mediated induction of *PUMA* gene expression through the nuclear-translocated p53 is not so much a question of cell-death inducing activity, but the GGA-induced disappearance of p53 from the cytoplasm may well be consistent with triggering autophagy. Kroemer's group noted that autophagy-inducing stimuli cause the depletion of cytoplasmic p53, which in turn is required for the induction of autophagy[35]. Whether the depletion of cytoplasmic p53 is necessary and sufficient for GGA-induced autophagy in HuH-7 cells has not yet been evaluated, though it is clear that both events occur within 3 h after GGA addition. Indeed, upon GGA treatment, PLC/PRF/5 cells continued to die even without induction of *PUMA*, suggesting that the up-regulation of *PUMA* expression is not essential for GGA-induced cell death. Unlike HepG2 cells, but similar to HuH-7 cells, PLC/PRF/5 cells showed a rapid nuclear translocation of the cytoplasmic p53 (Figure 2d) and a massive accumulation of autophagosomes (unpublished results) following GGA treatment, implying that a nuclear translocation of cytoplasmic p53 is important for GGA-induced autophagic cell death.

In conclusion, the present study clearly illustrates that GGA, a cancer-preventive acyclic diterpenoid, induces rapid nuclear translocation of cytoplasmic p53 in human hepatoma-derived HuH-7 cells and results in selective and dramatic upregulation of *PUMA* gene expression, which might be linked to cell death with accumulation of autophagosomes[19].

Methods

Cell culture and drug treatment. Human hepatoma-derived HuH-7 (p53 Y220C), PLC/PRF/5 (p53 R249S), and HepG2 (p53 WT) cells were cultured in Dulbecco's modified Eagle's medium (D-MEM) (Wako, Osaka, Japan) supplemented with 5% fetal bovine serum (FBS). Hep3B cells (p53 null) were maintained in D-MEM containing 10% FBS and MEM non-essential amino acid solution (Sigma Aldrich, St. Louis, MO, USA). HuH-7, HepG2, and PLC/PRF/5 cells were obtained from the RIKEN cell bank (Tsukuba, Japan) and Hep3B cells were from DS Pharma Biomedical (Osaka, Japan). The cells were cultured with D-MEM containing 5% or 10% FBS for 2 days and the medium was replaced with FBS-free D-MEM 1 day before GGA treatment. GGA was a generous gift from Kuraray Company (Okayama, Japan).

To block nuclear translocation of p53, HuH-7 cells were treated with ivermectin (Sigma Aldrich) at a concentration of 2.5 μM for 1 h before the treatment of 20 μM GGA supplemented with 2.5 μM ivermectin.

Transfection with small interfering RNA (siRNA). p53 siRNAs (sense: 5′ -AGA-CCU-AUG-GAA-ACU-ACU-Utt-3′) were purchased from FASMAC (Kanagawa, Japan). For transfection, HuH-7 cells were seeded on 3-cm dishes (Thermo Fisher Scientific, Nunc, Roskilde, Denmark) at a density of 3 or 5×10^4 cells/dish. Following incubation overnight, p53 siRNA or control siRNA-A (Santa Cruz Biotechnology, Santa Cruz, CA, USA) were transfected using Lipofectamine^R 2000 (Thermo Fischer Scientific, Invitrogen, Tokyo, Japan) according to the manufacturer's instructions. Following incubation for 96 h, the cells were treated with GGA (0–20 μM). After GGA treatment, viable cell counting was performed using the Trypan Blue dye-exclusion method (Sigma Aldrich).

Reverse-transcription real-time polymerase chain reaction (RT-qPCR). HuH-7, PLC/PRF/5, HepG2, and Hep3B cells were treated with GGA (final concentrations of 2.5–50 μM in medium) or vehicle alone, and total RNA was isolated using the QuickGene RNA Cultured Cell Kit S (Wako) with QuickGene-810 (Kurabo, Osaka, Japan). Complementary DNA was generated using the Transcriptor® First Strand cDNA Synthesis Kit with random hexamer (Roche Diagnostics, Basel, Switzerland). Nucleotide sequences of the PCR primers, including those for the *p21*, *PUMA*, *TIGAR*, *SCO2*, *DRAM*, and *28S rRNA* cDNAs, are listed in Supplementary Table S1. Real-time PCR was performed with DyNAmo^{TM} Capillary SYBR® Green qPCR Master mix (Finnzymes, Espoo, Finland), and cDNA on LightCycler1.5 (Roche Diagnostics) under conditions described in Supplementary Table S2.

Immunoblotting. After GGA (20 μM) treatment, HuH-7, PLC/PRF/5, HepG2, and Hep3B cells were lysed with RIPA buffer and proteins were quantified using the Bradford assay (Bio-Rad, Hercules, CA, USA). Equal amounts (5–30 μg) of protein were separated by SDS-PAGE and transferred to semi-dry blotted PVDF membranes (Bio-Rad). Membranes were probed with a mouse monoclonal antibody against p53 (Clone BP53-12, Sigma Aldrich), rabbit polyclonal antibodies against PUMA (ab54288, Abcam, Cambridge, UK), phospho-p53 (phosphorylated at Ser^{15}) (Ab-3, Calbiochem, Darmstadt, Germany), acetyl-p53 (acetylated at Lys^{379}) (#2570, Cell Signaling Technology, Boston, MA, USA), β-actin (#4967, Cell Signaling Technology), porin (Ab-5, Calbiochem), and β-III-tubulin (T2200, Sigma Aldrich). HRP (horseradish peroxidase)-labeled secondary antibodies were detected with Immobilon Western Chemiluminescent HRP substrate (Merck Millipore, Billerica, MA, USA) on an ImageQuant LAS 4000 (GE Healthcare, Tokyo, Japan).

Immunofluorescence. After 20 μM GGA or ethanol treatment, HuH-7 and PLC/PRF/5 cells on a glass insert in a 24-well plate were rinsed with PBS(−) and fixed for 40 min with 4% paraformaldehyde containing 2% sucrose in PBS(−) and then rinsed with PBS(−). The cells were permeated with 0.5% TritonX-100 and blocked with 10% FBS. The cells were then incubated at 4°C overnight with a monoclonal anti-p53 antibody (Cell Signaling Technology), followed by a 2.5-h incubation with an Alexa-488-labeled goat anti-mouse IgG antibody (Invitrogen, Molecular Probes, Tokyo, Japan). After rinsing with PBS(−), the cells were mounted in ParmaFluor (Beckman Coulter, Brea, CA, USA), covered on a slide glass, and observed under a confocal laser-scanning fluorescence microscope, an LSM700 2Ch URGB equipped with Axio Observer Z1 Bio (Carl Zeiss, Göttingen, Germany).

Subcellular fractionation and treatment with GGA. HuH-7 and HepG2 cells were washed on ice with ice-cold PBS(−), scraped off in PBS(−) and centrifuged at $500 \times g$ for 5 min. The resultant cell pellets were gently suspended with PBS(−) and homogenized with a Dounce-type homogenizer on ice. The cell lysates were centrifuged at $600 \times g$ for 14 min at 4°C to separate the nuclear fraction (pellet). The supernatant was centrifuged at $14\,300 \times g$ for 15 min at 4°C to obtain the post-mitochondrial fraction (supernatant), which contained other organelles smaller than mitochondria, such as microsomes (fragmented endoplasmic reticulum), peroxisomes and lysosomes, and cytosol. The washed pellet was re-suspended with PBS(−) as the mitochondrial fraction. The post-mitochondrial fraction was centrifuged at $105\,000 \times g$ and $348\,900 \times g$ for 90 min at 4°C. The supernatants from the two centrifugations were designated as the cytosolic fraction and $348\,900 \times g$ supernatant fraction, respectively.

GGA (final concentration of 0–20 μM) was added to each above-described subcellular fraction (10 μg protein each), and samples were vortexed and incubated overnight at 4°C under dark conditions until electrophoresis.

BN-gradient PAGE followed by immunoblotting. After overnight incubation with GGA (0–20 μM), samples were prepared with 4 × Native PAGE^{TM} Sample Buffer (Invitrogen) and subjected to electrophoresis at room temperature on 4–16% gradient Native PAGE Bis-Tris gels (Invitrogen) with a light-blue cathode buffer, according to the manufacturer's instructions. The separated proteins were blotted to a PVDF

membrane under semi-dry conditions. The proteins on the membranes were fixed with 8% acetic acid for 15 min, rinsed with deionized water, and briefly air-dried. The membranes were washed in methanol to remove excess Coomassie blue dye, rinsed with deionized water, shaken in PBS-T (PBS(−) containing 0.1% polyoxyethylene sorbitan monolaurate) for 5 min, blocked in 5% skim milk in PBS-T for 1 h at room temperature, and incubated overnight with an anti-p53 monoclonal antibody (Sigma Aldrich).

Cross-linking SDS-PAGE. Prior to addition of a cross-linking agent, the pH of the solutions containing samples from GGA (0–20 μM) treatment in cell-free experiments was adjusted between 6.5 and 7.5 with 2 M HCl. The samples were then incubated with a 0.04 mM BMH (bis(maleimido) hexane; Pearce Biotechnology, Rockford, IL, USA) cross-linker for 2 h at 4°C. The non-reacted cross-linking agent was then quenched with 42 mM dithiothreitol, and the samples were subjected to SDS-PAGE followed by immunoblotting analysis.

Co-immunoprecipitation. After treatment with GGA (0–20 μM), the samples were incubated with normal rabbit IgG or the polyclonal anti-PARC antibody at 4°C for 1 h with gentle mixing. The immune complexes were precipitated with EZview Red Protein G Affinity Gel beads (Sigma Aldrich), which were pre-washed with PBS(−) twice for 1 h at 4°C with gentle mixing. The nonspecifically bound proteins were removed by washing the beads with PBS(−) three times at 4°C. The beads in PBS(−) were centrifuged for 30 s at 8 200 *g*. The pellet was resuspended with 25 μl of PBS(−) and 2 × sample buffer, and the samples (10 μl) were subjected to SDS-PAGE and immunoblotting analysis.

Dual luciferase assay. HuH-7 cells were seeded in 96-well plates 1 day before transfection. Either the Cignal p53 reporter vector containing a p53-responsive consensus sequence (100 ng/well; Qiagen, Tokyo, Japan) or the PUMA Frag1-luciferase vector containing the p53-responsive 5′-upstream regulatory region of the *PUMA* gene (120 ng/well; Addgene, Cambridge, MA, USA) and the pRL-SV40 control vector (3 ng/well; Promega, Tokyo, Japan) were co-transfected using Lipofectamine 2000 and cells were incubated overnight. The cells were treated with GGA (0–20 μM) after transfection, and firefly and renilla luciferase activities were analysed by the Dual-Luciferase Reporter Assay System (Promega). The intensity of chemiluminescence was measured with CentroXS^3 (Berthold Technologies Japan, Tokyo, Japan).

1. Muller, P. A., Vousden, K. H. & Norman, J. C. p53 and its mutants in tumor cell migration and invasion. *J. Cell Biol.* **192**, 209–218 (2011).
2. Cheok, C. F., Verma, C. S., Baselga, J. & Lane, D. P. Translating p53 into the clinic. *Nat. Rev. Clin. Oncol.* **8**, 25–37 (2011).
3. Bensaad, K. & Vousden, K. H. p53: new roles in metabolism. *Trends Cell Biol.* **17**, 286–291 (2007).
4. Yu, J. & Zhang, L. PUMA, a potent killer with or without p53. *Oncogene* **27 Suppl 1**, S71–83 (2008).
5. Yee, K. S., Wilkinson, S., James, J., Ryan, K. M. & Vousden, K. H. PUMA- and Bax-induced autophagy contributes to apoptosis. *Cell Death Differ.* **16**, 1135–1145 (2009).
6. Brown, C. J., Cheok, C. F., Verma, C. S. & Lane, D. P. Reactivation of p53: from peptides to small molecules. *Trends Pharmacol. Sci.* **32**, 53–62 (2011).
7. Li, D. *et al.* Functional inactivation of endogenous MDM2 and CHIP by HSP90 causes aberrant stabilization of mutant p53 in human cancer cells. *Mol. Cancer Res.* **9**, 577–588 (2011).
8. Kaustov, L. *et al.* The conserved CPH domains of Cul7 and PARC are protein-protein interaction modules that bind the tetramerization domain of p53. *J. Biol. Chem.* **282**, 11300–11307 (2007).
9. Pei, X. H. *et al.* Cytoplasmic CUL9/PARC ubiquitin ligase is a tumor suppressor and promotes p53-dependent apoptosis. *Cancer Res.* **71**, 2969–2977 (2011).
10. Vousden, K. H. & Ryan, K. M. p53 and metabolism. *Nat. Rev. Cancer* **9**, 691–700 (2009).
11. Crighton, D. *et al.* DRAM, a p53-induced modulator of autophagy, is critical for apoptosis. *Cell* **126**, 121–134 (2006).
12. Mah, L. Y., O'Prey, J., Baudot, A. D., Hoekstra, A. & Ryan, K. M. DRAM-1 encodes multiple isoforms that regulate autophagy. *Autophagy* **8**, 18–28 (2012).
13. Maiuri, M. C. *et al.* Autophagy regulation by p53. *Curr. Opin. Cell Biol.* **22**, 181–185 (2010).
14. Shidoji, Y. & Ogawa, H. Natural occurrence of cancer-preventive geranylgeranoic acid in medicinal herbs. *J. Lipid Res.* **45**, 1092–1103 (2004).
15. Sano, T. *et al.* Prevention of rat hepatocarcinogenesis by acyclic retinoid is accompanied by reduction in emergence of both TGF-alpha-expressing oval-like cells and activated hepatic stellate cells. *Nutr. Cancer* **51**, 197–206 (2005).
16. Okusaka, T., Ueno, H., Ikeda, M. & Morizane, C. Phase I and pharmacokinetic clinical trial of oral administration of the acyclic retinoid NIK-333. *Hepatol. Res.* **41**, 542–552 (2011).
17. Muto, Y. *et al.* Prevention of second primary tumors by an acyclic retinoid, polyprenoic acid, in patients with hepatocellular carcinoma. Hepatoma Prevention Study Group. *N. Engl. J. Med.* **334**, 1561–1567 (1996).
18. Shidoji, Y., Nakamura, N., Moriwaki, H. & Muto, Y. Rapid loss in the mitochondrial membrane potential during geranylgeranoic acid-induced apoptosis. *Biochem. Biophys. Res. Commun.* **230**, 58–63 (1997).
19. Okamoto, K., Sakimoto, Y., Imai, K., Senoo, H. & Shidoji, Y. Induction of an incomplete autophagic response by cancer-preventive geranylgeranoic acid (GGA) in a human hepatoma-derived cell line. *Biochem. J.* **440**, 63–71 (2011).
20. Beghin, A., Matera, E. L., Brunet-Manquat, S. & Dumontet, C. Expression of Arl2 is associated with p53 localization and chemosensitivity in a breast cancer cell line. *Cell Cycle* **7**, 3074–3082 (2008).
21. Azmi, A. S. *et al.* Reactivation of p53 by novel MDM2 inhibitors: implications for pancreatic cancer therapy. *Curr. Cancer Drug Targets* **10**, 319–331 (2010).
22. Nikolaev, A. Y., Li, M., Puskas, N., Qin, J. & Gu, W. Parc: a cytoplasmic anchor for p53. *Cell* **112**, 29–40 (2003).
23. Trostel, S. Y., Sackett, D. L. & Fojo, T. Oligomerization of p53 precedes its association with dynein and nuclear accumulation. *Cell Cycle* **5**, 2253–2259 (2006).
24. Shimonishi, S. *et al.* Rapid downregulation of cyclin D1 induced by geranylgeranoic acid in human hepatoma cells. *Nutr. Cancer* **64**, 473–480 (2012).
25. Wagstaff, K. M., Sivakumaran, H., Heaton, S. M., Harrich, D. & Jans, D. A. Ivermectin is a specific inhibitor of importin alpha/beta-mediated nuclear import able to inhibit replication of HIV-1 and dengue virus. *Biochem. J.* **443**, 851–856 (2012).
26. Woo, M. G., Xue, K., Liu, J., McBride, H. & Tsang, B. K. Calpain-mediated processing of p53-associated parkin-like cytoplasmic protein (PARC) affects chemosensitivity of human ovarian cancer cells by promoting p53 subcellular trafficking. *J. Biol. Chem.* **287**, 3963–3975 (2012).
27. Giustiniani, J. *et al.* Tubulin acetylation favors Hsp90 recruitment to microtubules and stimulates the signaling function of the Hsp90 clients Akt/PKB and p53. *Cell Signal.* **21**, 529–539 (2009).
28. Wiech, M. *et al.* Molecular mechanism of mutant p53 stabilization: the role of HSP70 and MDM2. *PLoS One* **7**, e51426, DOI: 10.1371/journal.pone.0051426 (2012).
29. Jin, S. *et al.* Gadd45a contributes to p53 stabilization in response to DNA damage. *Oncogene* **22**, 8536–8540 (2003).
30. Bhattacharya, S., Chaum, E., Johnson, D. A. & Johnson, L. R. Age-related susceptibility to apoptosis in human retinal pigment epithelial cells is triggered by disruption of p53-Mdm2 association. *Invest. Ophthalmol. Vis. Sci.* **53**, 8350–8366 (2012).
31. Shidoji, Y. *et al.* Prevention of geranylgeranoic acid-induced apoptosis by phospholipid hydroperoxide glutathione peroxidase gene. *J. Cell. Biochem.* **97**, 178–187 (2006).
32. Fen, C. X., Coomber, D. W., Lane, D. P. & Ghadessy, F. J. Directed evolution of p53 variants with altered DNA-binding specificities by in vitro compartmentalization. *J. Mol. Biol.* **371**, 1238–1248 (2007).
33. Joerger, A. C. & Fersht, A. R. Structure-function-rescue: the diverse nature of common p53 cancer mutants. *Oncogene* **26**, 2226–2242 (2007).
34. Bullock, A. N., Henckel, J. & Fersht, A. R. Quantitative analysis of residual folding and DNA binding in mutant p53 core domain: definition of mutant states for rescue in cancer therapy. *Oncogene* **19**, 1245–1256 (2000).
35. Morselli, E. *et al.* Mutant p53 protein localized in the cytoplasm inhibits autophagy. *Cell Cycle* **7**, 3056–3061 (2008).

Acknowledgments

We thank Ms. Seiko Kobayashi, a former graduate student, who produced preliminary data on nuclear translocation of p53 and upregulation of *PUMA* gene expression after GGA treatment. This work was supported in part by a grant-in-aid from the Japan Society for the Promotion of Science (grant number19590230) and a research grant B from the University of Nagasaki.

Author contributions

Y.S. conceived the experimental design, analysed the raw data and wrote the main manuscript text and C.I. produced all experimental data, processed the data and wrote the materials & methods and results sections, and prepared all figures and tables. All authors reviewed the manuscript.

Additional information

Support: This work was supported in part by a grant-in-aid from the Japan Society for the Promotion of Science (grant number 19590230) and a research-grant B from the University of Nagasaki.

Supplementary information accompanies this paper at http://www.nature.com/scientificreports

Competing financial interests: The authors declare no competing financial interests.

How to cite this article: Iwao, C. & Shidoji, Y. Induction of nuclear translocation of mutant cytoplasmic p53 by geranylgeranoic acid in a human hepatoma cell line. *Sci. Rep.* **4**, 4419; DOI:10.1038/srep04419 (2014).